

## Formation of a rectifier with gold nanoclusters: X-ray reflectivity and atomic force microscopy measurements

S. Pal and M. K. Sanyal

*Surface Physics Division, Saha Institute of Nuclear Physics, 1/AF, Bidhannagar, Kolkata 700064, India*

Neena S. John and G. U. Kulkarni

*Chemistry and Physics of Materials Unit, Jawaharlal Nehru Center for Advanced Scientific Research, Jakkur, Bangalore-560064, India*

(Received 4 January 2005; revised manuscript received 18 February 2005; published 24 March 2005)

We demonstrate that monolayer and bilayer films of thiol-capped gold nanoclusters can exhibit prominent rectification properties, provided spatial asymmetry exists between the two tunnel junctions used to connect the nanoclusters. Systematic x-ray reflectivity and atomic force microscopy (AFM) measurements were carried out to characterize the spatial asymmetry introduced by a monolayer of fatty acid salt used to deposit thiol-capped gold nanoclusters on a hydrophilic  $\text{SiO}_2$ - $\text{Si}(001)$  substrate using the Langmuir–Blodgett technique. Current-voltage characteristics, obtained from conducting probe AFM measurements, show rectification ratios of 13.5 and 364.8 for the monolayer and bilayer films, respectively.

DOI: 10.1103/PhysRevB.71.121404

PACS number(s): 68.55.-a, 73.40.Gk, 73.63.Bd

Nanomaterial-based rectifiers will be an important ingredient in nanotechnology and the simplest application of these rectifiers will be in memory devices with enormous storage capacity.<sup>1</sup> The present status of this field is, however, not suitable for immediate technological applications demanding sharp voltage thresholds, large current rectification ratios, small time constants, and above all, easy-to-form stable molecular structure. Experimental and theoretical studies of current-voltage ( $I$ - $V$ ) characteristics of monomolecular films are being carried out extensively to achieve such desired properties and these studies also improve our basic understanding of the electrical transport phenomena in low dimension. The original concept<sup>2</sup> of molecular rectifier (MR) was developed with the assumption that highest occupied molecular orbital (HOMO) and lowest unoccupied molecular orbital (LUMO) can be confined in two parts of a molecule separated by an insulator bridge that prevents orbital overlap or “spilling off” forming a donor-insulator-acceptor ( $D$ - $\sigma$ - $A$ ) structure. Monomolecular film of a zwitterionic molecule grown by Langmuir-Blodgett (LB) technique exhibited rectification properties,<sup>3</sup> but extensive experiments have shown<sup>4,5</sup> that the molecule is actually donor- $\pi$ -electron bridge-acceptor ( $D$ - $\pi$ - $A$ ) and not a  $D$ - $\sigma$ - $A$  structure.

It is now realized<sup>4-6</sup> that having an insulator ( $\sigma$ ) bridge within a molecule may be questionable in most cases and one can form rectifiers easily by connecting a molecule asymmetrically to two tunnel barriers from each side in a line of sight. In this situation one can in principle design a rectifier by altering the spatial asymmetry of the connecting tunnel barriers.<sup>1,6-8</sup> Here, we demonstrate that one can form a rectifier using a dodecanethiol capped gold nanocluster (3.3-nm diam) held in an asymmetric spatial configuration with thiol chains on one side and a layer of gadolinium stearate on  $\text{SiO}_2$ - $\text{Si}$  substrate, on the other. Although electrical properties of metal nanoclusters connected by organic tails are being studied rigorously,<sup>9-12</sup> so far a rectifier functionality from such nanocluster systems has not been reported.

A schematic diagram of the nanocluster assembly is

shown in Fig. 1(a) along with the connections used for the  $I$ - $V$  measurements on a conducting probe atomic force microscope (C-AFM). The films were deposited in an LB trough on a native-oxide-covered doped Si (001) substrate through a sequential process involving two water-to-air strokes. The substrate cleaning and other details have been described earlier.<sup>13</sup> In the first stroke the substrate was taken through a compressed Langmuir monolayer of stearic acid having gadolinium ions in the water subphase forming a gadolinium stearate (GdSt) monolayer on a hydrophilic  $\text{SiO}_2$ - $\text{Si}$  substrate. Then, this hydrophobic GdSt- $\text{SiO}_2$ - $\text{Si}$  substrate was again taken from water to air through a Langmuir monolayer of dodecanethiol encapsulated Au nanoclusters forming the second monolayer on GdSt. The presence of the GdSt monolayer improves the film quality and the third monolayer can be formed on the substrate if the surface pressure of the Langmuir monolayer of Au nanoclusters is kept higher.<sup>13</sup> In this communication, we present our investigations on the electrical properties of two films marked *A* and *B*, deposited with surface pressures of 1.5 and 20.0 mN/m resulting in, respectively, a monolayer and bilayer of Au nanoclusters on GdSt- $\text{SiO}_2$ - $\text{Si}$  substrates. With spatial configuration being the key feature of this study, we determined the morphology and thickness of the films using x-ray reflectivity and AFM as two independent measurements. The  $I$ - $V$  characteristics of films *A* and *B*, as well as of GdSt- $\text{SiO}_2$ - $\text{Si}$  and the bare  $\text{SiO}_2$ - $\text{Si}$  substrate, were measured using the conducting probe AFM setup (Nanoscope IV, Digital Instruments) with a gold-coated  $\text{Si}_3\text{N}_4$  tip.<sup>14</sup> In order to confirm diode-like properties observed in C-AFM measurements, we have also measured  $I$ - $V$  characteristic of the films by two-probe technique using an electrometer (Keithley 6517A).

In Fig. 1(b) we have shown x-ray reflectivity profiles of films *A* and *B*, and GdSt- $\text{SiO}_2$ - $\text{Si}$  substrates. The electron density profiles (EDPs) (shown in the insets) are extracted by fitting,<sup>13</sup> and the fitted reflectivity profiles are also shown with measured data. Electron density profiles of the films and

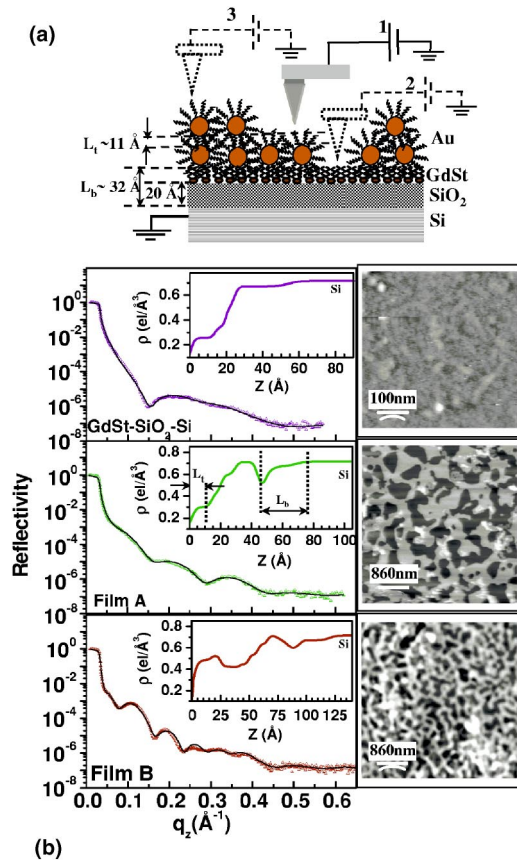


FIG. 1. (Color online) (a) Schematic diagram of the Au nanocluster film on GdSt-SiO<sub>2</sub>-Si substrate along with the electrical connection for C-AFM measurements. Three tip positions are shown on the (1) monolayer of Au nanoparticles (2) GdSt-SiO<sub>2</sub>-Si substrate, and (3) bilayer of Au nanoparticles. (b) X-ray reflectivity data (scatter graphs) along with the fitted profiles (solid lines) for samples A and B, and the GdSt-SiO<sub>2</sub>-Si substrate. Corresponding electron density profiles (EDPs) are shown in the insets and corresponding tapping mode AFM images are shown in the right panel. The length scales obtained from x-ray analysis are marked in EDPs and also in (a). The top and bottom barrier widths ( $L_t$  and  $L_b$ , respectively) are shown in EDP of film A.

measured AFM morphology of the films [also shown in Fig. 1(b)] were used to determine<sup>13</sup> the distances accurately (within  $\pm 2$  Å) as indicated in the simplified model shown in Fig. 1(a). With a native SiO<sub>2</sub> thickness of 20 Å an asymmetric spatial tunnel barrier is apparent even in film A having primarily a monolayer of Au clusters on the GdSt-SiO<sub>2</sub>-Si substrate. The C-AFM tip is about 11-Å away from the Au cluster and the other conducting connection of doped Si (001) is around 32 Å (=20 Å for SiO<sub>2</sub>+12 Å for thiols and GdSt layer) away. This spatial asymmetry gives rise to diode-like  $I$ - $V$  characteristics in C-AFM measurements provided the tip is placed on the top of an Au cluster. The separation (12 Å) of the Au cluster and SiO<sub>2</sub>-Si interface is much less than the expected thickness of thiol plus stearic acid tails (14+20=34 Å) indicating rearrangements of organic tails below the Au cluster.

We have shown a C-AFM tip position [point 1 in Figs. 2(a) and 1(a)] on film A and the corresponding  $I$ - $V$  charac-

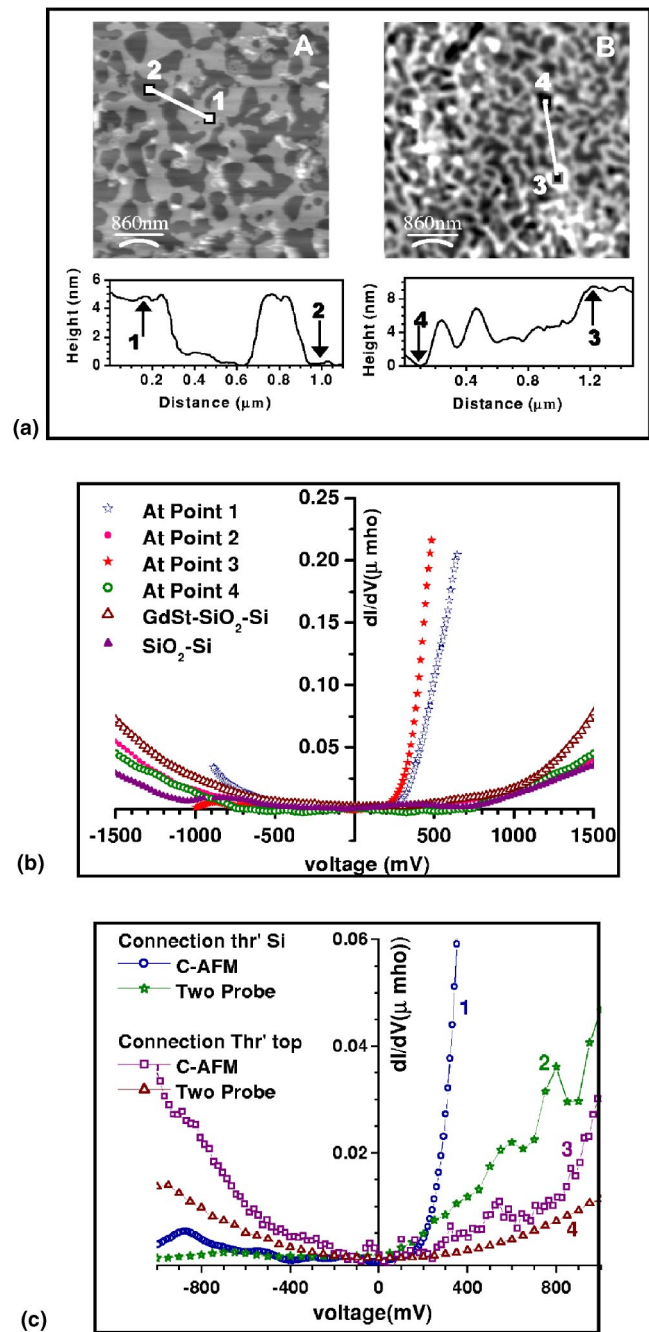


FIG. 2. (Color online) (a) AFM images of films A and B along with the corresponding height profiles. The tip positions for  $I$ - $V$  measurements are marked in the images and also in the profiles. (b)  $dI/dV$  vs  $V$  plots for samples A and B, the GdSt-SiO<sub>2</sub>-Si substrate, and bare SiO<sub>2</sub>-Si. Four curves are shown for samples A and B corresponding to four marked tip positions. (c)  $dI/dV$  vs  $V$  plots obtained from C-AFM and two-probe measurements by taking the second connections from the back side of Si substrate (curves 1 and 2) and from film (curves 3 and 4) (refer to text for details).

teristics of this Au cluster in Fig. 2(b) as conductance ( $dI/dV$ ) plot as a function of voltage applied to the tip. We observe a sharp rise in conductance beyond a forward voltage ( $V_F$ ) of +240 mV but reverse voltage  $V_R$  comes out to be around -450 mV for obtaining nonzero conductance. The

current rectification ratio ( $R$ ), which is the ratio of forward to reverse currents at a given magnitude of the bias, at  $\pm 500$  mV is estimated to be 13.5. Interestingly, a symmetric behavior is observed with  $R$  nearly close to unity when the tip is not placed on the Au cluster [point 2 in Figs. 2(a) and 1(a)]. The tip is now on the GdSt layer as evident from the height profile of Fig. 2(a) and obtained conductance versus voltage is similar to that obtained by measuring the bare GdSt-SiO<sub>2</sub>-Si substrate shown in Fig. 2(b). This observation also indicates that tail distortion takes place only below an Au cluster. In Fig. 2(b) we have also shown measured conductance spectra of bare SiO<sub>2</sub>-covered doped Si (001) substrate used in this experiment. The symmetric profile observed here is typical tunneling data through a SiO<sub>2</sub> barrier that depend strongly on tip separation.<sup>7</sup>

The spatial asymmetry becomes more prominent for film *B* provided the tip is placed on a bilayer of Au nanocluster [point 3 in Figs. 2(a) and 1(a)]. In this condition we could not get conductance in the negative voltage side and conductance in the positive voltage side remains similar but slightly better [Fig. 2(b)] and  $R$  comes out to be 364.8. In this film also we get back a conductance profile [refer to Fig. 2(b)] of GdSt-SiO<sub>2</sub>-Si if the tip is placed on GdSt [point 4 in Fig. 2(a)] that is around 90-Å below the top Au nanocluster as shown in the height profile. Moreover, we get back a conductance profile of an Au nanocluster of film *A* by positioning the tip [point 1 in Fig. 1(a)] on an Au cluster situated in the first monolayer of film *B*. This result confirms that in-plane conduction through Au nanoclusters is not dominating here. The results in Fig. 2(b) clearly demonstrate that dominating current-carrying paths here are tunneling through a C-AFM tip-to-Au nanocluster-to-doped Si structure, and one can produce rectifiers even with thiol-capped Au clusters having a diameter of 3.3 nm.

This rectifying characteristic of films *A* and *B* is not observed when the connection is taken from the film itself, avoiding a tunneling barrier of SiO<sub>2</sub> as we had reported earlier.<sup>13</sup> We present here standard two-probe conductance data to illustrate the role of asymmetry further. Two-probe measurements were performed with an electrometer by making one connection with a conducting pad from the top of the film—the other connection was taken either from another portion of film [curve 4 in Fig. 2(c)] or from the back of the Si substrate [curve 2 in Fig. 2(c)]. Curve 1 in Fig. 2(c) is the same as the data of point 1 shown in Fig. 2(b) and can be used as a reference. The rectification is evident even in two-probe data when a connection is taken from the back of the substrate [curve 2 of Fig. 2(c)], but the contrast is less as the conducting pad averages the conductance of the Au nanocluster with that of GdSt due to the patchy nature of the Au cluster monolayer [refer to Fig. 2(a)]. However, the rectification feature does not appear in both C-AFM and two-probe data shown as curves 3 and 4, respectively, in Fig. 2(c) when the other connection is taken from the film-avoiding SiO<sub>2</sub> interface.

The diode-like property of the Au nanocluster observed here can be explained on the basis of spatial asymmetry in two tunnel barriers—one formed by organic tails of thiol molecules lying between a C-AFM tip and Au nanocluster (top barrier of thickness  $L_t = 11$  Å), and the other formed by

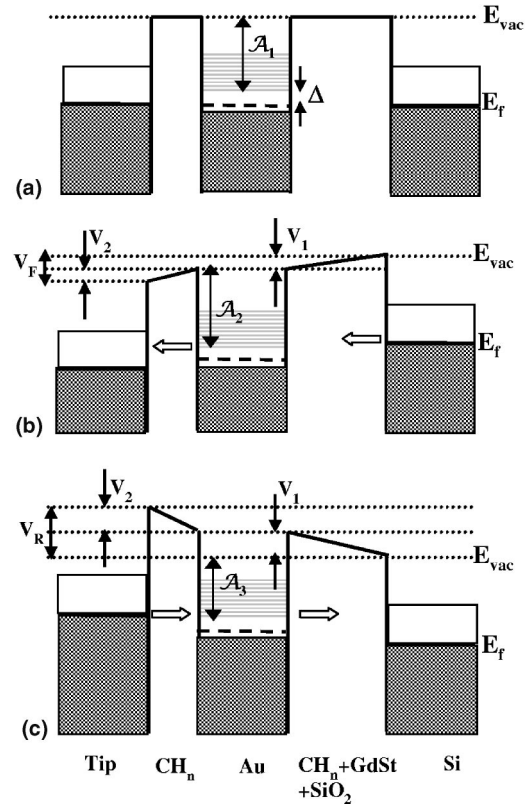


FIG. 3. (a) Schematic diagram showing the asymmetric tunnel barriers. Fermi levels are aligned at zero bias. (b) At a positive bias ( $V_F$ ) to tip, the Si Fermi level lines up with the conduction level of the Au nanocluster. (c) At a negative bias ( $V_R$ ) to tip, the tip Fermi level aligns with the conduction level of the Au cluster. The voltage drops across the top and bottom barriers, and the electron affinity of the Au cluster is marked as  $V_t$ ,  $V_b$ , and  $A_t$ , respectively.

a thiol-GdSt-SiO<sub>2</sub> barrier in between an Au nanocluster and Si (bottom barrier of thickness  $L_b = 32$  Å). The applied voltage,  $V$ , drops asymmetrically on the top and bottom barriers giving rise to a diode-like property as expected.<sup>1,6,7</sup> Let the voltage drop at the bottom and top barriers be  $V_b$  and  $V_t$ , respectively, with their ratio  $\eta = V_b/V_t$ . In the schematic diagram (Fig. 3) we do not show the band gap of the *n*-type (carrier concentration  $\sim 1.6 \times 10^{17}$  cm<sup>-3</sup>) Si(001) used here explicitly and to the first approximation we treat the doped Si as a metallic electrode.<sup>15</sup> At equilibrium the Fermi levels of the C-AFM tip and Si align with the Fermi level of an Au nanoparticle as shown in Fig. 3(a). The equilibrium Fermi level position obviously depends on the relative work functions of the two electrodes, which are not the same in our case. The difference in work functions induces a contact potential difference and hence an electric field through the system at zero applied bias. For simplicity we ignore the field within the nanocluster and assume that the applied voltage drops only on the two barriers, i.e.,  $V = V_b + V_t$ . In our diagram, the bottom electrode (Si) is always grounded and all the energy levels shift with respect to the Si Fermi level with applied bias. From density-functional studies it has been shown earlier<sup>16</sup> that a thiol-passivated Au cluster consisting of 38 Au atoms has a gap of 0.9 eV just above the Fermi energy. We denote this gap as  $\Delta = (E_{vac} - E_f) - A_1$ , where  $E_{vac}$ ,

$E_f$ , and  $A_1$  are the vacuum level, equilibrium Fermi level position, and electron affinity of Au nanoparticle at zero bias, respectively.

When the positive voltage is applied to the tip, the tip Fermi energy and the energy levels of the Au nanocluster shift downward, but their relative shifting will depend on  $\eta$ . At a particular forward bias voltage ( $V_F$ ) the Si Fermi level lines up with the conduction levels of the Au nanocluster [Fig. 3(b)] and a sharp increase in current is observed in  $I$ - $V$  spectra due to resonant tunneling.<sup>6,7</sup> Similarly, in reverse bias both the tip Fermi energy and the energy levels of the Au cluster shift upwards and current will start to increase at a voltage ( $V_R$ ) only when the tip Fermi level lines up with the conduction levels of the Au cluster [Fig. 3(b)]. From the expressions<sup>6</sup>  $eV_F = \Delta(1 + \eta)/\eta$  and  $eV_R = \Delta(1 + \eta)$ , the asymmetric factor  $\eta = V_R/V_F$  is found to be 1.9 for sample A. For sample B, current is almost zero in negative bias giving  $\eta \gg 1$ . From the above expressions  $\Delta$  is found out to be 155 meV. This is consistent with earlier reports<sup>17,18</sup> which mentioned that the HOMO-LUMO gap present in a thiol-capped Au nanocluster of 0.5 and 2-nm diam is 1.8 and 0.3 eV, respectively. Here we should mention that the asymmetric parameter (denoted as  $\eta'$  here) introduced by Tian *et al.*<sup>7</sup> differs from the definition of  $\eta$  used here.<sup>6</sup> From definition one can easily relate  $\eta$  with  $\eta'$  ( $=V_t/V$ ) as  $\eta = (1 - \eta')/\eta'$  and  $\eta'$  is found to be 0.34 for sample A. The asymmetric factor  $\eta$  can be approximated<sup>7,19</sup> in terms of the parallel-plate capacitances of the two junctions using a simple dielectric model with the widths and relative dielectric constants of the top and bottom barriers  $L_t$ ,  $L_b$ ,  $\epsilon_t$ , and  $\epsilon_b$ , respectively. Assuming further that the area associated with

the tunneling phenomena for the two barriers is the same, one can write  $\eta = (L_b/L_t)(\epsilon_t/\epsilon_b)$ . Considering  $L_b = 32$  Å,  $L_t = 11$  Å, and  $\epsilon_t = 2.2$ , which is the commonly used<sup>10</sup> value for alkane chains,  $\epsilon_b$  comes out to be 3.3. The dielectric constant of the bottom barrier is expected to be higher than the top one because of the presence of SiO<sub>2</sub>. By keeping only organic tails on both sides of Au nanoclusters one can get higher  $\eta$  and hence better R.

We have demonstrated that monolayer and bilayer films of thiol-capped Au nanoclusters deposited on GdSt-SiO<sub>2</sub>-Si substrate can exhibit rectification properties when the film is asymmetrically coupled to two electrodes. The spatial asymmetry introduced by the different widths of the tunnel barriers at the top and bottom sides of the film plays the key role in generating the asymmetric  $I$ - $V$  curves. An obvious extension of our finding is that one can create an array of rectifiers by depositing thiol-capped Au nanoclusters on an organic monolayer attached to a doped silicon or metal substrate. The rectification ratio can then be designed by choosing the desired “tail length” of the organic monolayer. We also plan to extend these measurements using both  $n$ - and  $p$ -type Si substrate at low temperature to understand the role of energy gaps<sup>6</sup> of the electrodes in determining the rectifier properties.

The authors would like to acknowledge the help of Atikur Rahman in two-probe measurements and the help of V. Venkataraman, O.V.S.N. Murthy, and Subhendu Sarkar in characterizing the silicon substrate. The authors are also grateful to Professor C. N. R. Rao for his support in this collaboration. N. S. J. would like to thank CSIR for financial assistance.

- 
- <sup>1</sup>D. M. Adams *et al.*, J. Phys. Chem. B **107**, 6668 (2003).  
<sup>2</sup>A. Aviram and M. A. Ratner, Chem. Phys. Lett. **29**, 277 (1974).  
<sup>3</sup>A. S. Martin, J. R. Sambles, and G. J. Ashwell, Phys. Rev. Lett. **70**, 218 (1993).  
<sup>4</sup>R. M. Metzger, T. Xu, and I. R. Peterson, J. Phys. Chem. B **105**, 7280 (2001).  
<sup>5</sup>R. M. Metzger, B. Chen, U. Höpfner, M. V. Lakshmikantham, D. Vuillaume, T. Kawai, X. Wu, H. Tachibana, T. V. Hughes, H. Sakurai, J. W. Baldwin, C. Hosch, M. P. Cava, L. Brehmer, and G. J. Ashwell, J. Am. Chem. Soc. **119**, 10455 (1997).  
<sup>6</sup>P. E. Kornilovitch, A. M. Bratkovsky, and R. S. Williams, Phys. Rev. B **66**, 165436 (2002).  
<sup>7</sup>W. Tian, S. Datta, S. Hong, R. Reifenberger, J. I. Henderson, and C. P. Kubiak, J. Chem. Phys. **109**, 2874 (1998).  
<sup>8</sup>S. Lenfant, C. Krzeminski, C. Delerue, G. Allan, and D. Vuillaume, Nano Lett. **3**, 741 (2003).  
<sup>9</sup>K.-H. Muller, J. Herrmann, B. Raguse, G. Baxter, and T. Reda, Phys. Rev. B **66**, 075417 (2002).  
<sup>10</sup>K.-H. Muller, G. Wei, B. Raguse, and J. Myers, Phys. Rev. B **68**, 155407 (2003).  
<sup>11</sup>C. T. Black, C. B. Murray, R. Sandstrom, and L. S. Sun, Science **290**, 1131 (2000).  
<sup>12</sup>R. Parthasarathy, X.-M. Lin, K. T. Elteto, T. F. Rosenbaum, and H. M. Jaeger, Phys. Rev. Lett. **92**, 076801 (2004).  
<sup>13</sup>S. Pal, N. S. John, P. J. Thomas, G. U. Kulkarni, and M. K. Sanyal, J. Phys. Chem. B **108**, 10770 (2004).  
<sup>14</sup>We also cross-checked  $I$ - $V$  characteristics of the GdSt-SiO<sub>2</sub>-Si system by approaching the C-AFM tip in the “holes” [tip position 2 in Fig. 1(a)] while measuring films A and B to ensure that characteristic of the GdSt-SiO<sub>2</sub>-Si structure had remained almost unaltered if it is not covered with Au nanoclusters in the last stroke of LB deposition.  
<sup>15</sup>In the GdSt-SiO<sub>2</sub>-Si system the effect of band bending and the presence of surface states in the Si gap region make it difficult to locate the valence- and conduction-band edge accurately with respect to the Fermi level.  
<sup>16</sup>H. Häkkinen, R. N. Barnett, and U. Landman, Phys. Rev. Lett. **82**, 3264 (1999).  
<sup>17</sup>C. N. R. Rao, G. U. Kulkarni, P. J. Thomas, and P. P. Edwards, Chem. Eur. J. **8**, 28 (2002).  
<sup>18</sup>O. D. Häberlen, Sai-Cheong Chung, M. Stener and N. Rosch, J. Chem. Phys. **106**, 5189 (1997).  
<sup>19</sup>C. Krzeminski, C. Delerue, G. Allan, D. Vuillaume, and R. M. Metzger, Phys. Rev. B **64**, 085405 (2001).